



A critical review of fracture mechanics as a tool for multiaxial fatigue life prediction of plastics¹

Anders Winkler, SPE, Gertjan Kloosterman

Dassault Systemes AB

anders.winkler@3ds.com, gertjan.kloosterman@3ds.com

ABSTRACT. Plastics belong to the most complex and probably least understood engineering materials of today. Combining the best aspects of design, mechanical properties and manufacturing, the structural integrity of plastics is on par with aluminium and can in some cases even rival those of steels. One of the most important aspects of plastics is the ability to tailor-drive their material properties for a specific purpose or towards a specific strength value. The morphology of plastics is directly dependent on the manufacturing process, e.g. injection moulding, extruding and casting. Plastics contain multiple phases (crystalline, amorphous, oriented), and are in no sense at all isotropic, although integrally deduced mechanical properties may appear to claim the opposite. As such, it becomes obvious that attempting to analyse such materials using conventional material models and explanations of mechanics is an inherently complex task. The static situation alone requires concepts such as creep, relaxation and rate effects to be incorporated on a numerical level. If the load situation changes, such that cyclic loading is acting on the continuum, with the morphology taken into account (without considering the actual geometrical shape), then the result is that of a complex multiaxial fatigue case. Classical theories used for treating fatigue such as SN or eN analysis have proven much less successful for plastics than they have for metals. Fatigue crack propagation using fracture mechanics has seen some success in application, although appropriate crack initiation criteria still need to be established. The physical facts are more than intriguing. For injection moulded parts (being the most common manufacturing process in place), fracture is in most cases seen to initiate from inside the material, unless the surface has been mechanically compromised. This appears to hold true regardless of the load case. In this review, we have scrutinised physically useful methods of crack initiation, as well as the use of fracture mechanics for multiaxial fatigue life prediction of injection-moulded plastics. Numerical tools have been utilised alongside experimental experience and public domain data to offer what we hope will be a contemporary overview, and offer an outlook for future research into the matter.

KEYWORDS. Plastics; Fracture mechanics; Temperature-dependent; Morphology; Structure; Manufacturing.

¹ *Disclaimer: All statements are strictly based on the authors' opinions. Dassault Systèmes and its affiliates disclaim any liability, loss, or risk incurred as a result of the use of any information or advice contained in this article, either directly or indirectly.*

INTRODUCTION

Plastics are in terms of engineering history relatively young materials. Compared to the amount of research available for metals, the inventions of pioneers such as Leo Baekland², Wallace Carothers³ and Stephanie Kwolek⁴ have barely had the tip of the proverbial ice berg scraped off. It is therefore no wonder that literature in this field is being updated at a rapid pace. Despite this, most material models for plastics in FEA are created from a phenomenological point of view and even then they are extremely difficult to calibrate. For fatigue, matters are even worse, where attempts to classify fatigue of plastics have not strayed far from modified SN analysis with very mixed results. When working with these types of materials it is important to begin from a point of trying to understand the linguistic origins of the terminology used in technical correspondence. It may at first seem odd to begin the treatment of an engineering field from a humanist point of view, but the benefit will become clear in an organic fashion. The words polymers and plastics are often used incorrectly, leading to inevitable confusion at an early stage in one of the most complex engineering fields. The word *polymer* is a compound of the two greek words *poli* (meaning many) and *meros* (meaning parts). A polymer can therefore simply be thought of as a material consisting of multiple building blocks. The word *plastics* refers to polymers which can be shaped or moulded in a manufacturing process into a large variety of geometric shapes. To summarize somewhat simplistically: all plastics are polymers, but not all polymers are plastics. Fig. 1 depicts a schematic representation of how ethylene monomers form polyethylene macromolecules through polymerization.

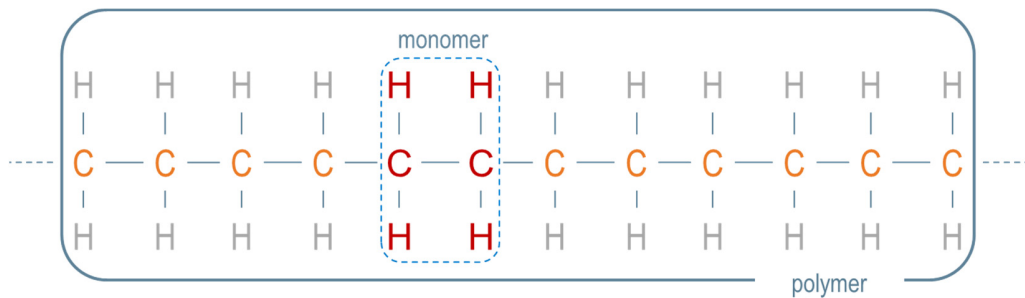


Figure 1: Schematic formation of PolyEthylene (PE) molecules.

THE PHYSICAL AND CHEMICAL STRUCTURE OF POLYMERS

The following section provides a basic overview of the physical and chemical structure of polymer materials. We believe that having some understanding of these structures will lead to an improved understanding why some algorithms will be better suited than others. The intent is not to cover this topic in great detail, as it does not fit the scope of this publication. The curious reader is instead referred to sources such as [1–6] for an extensive coverage of polymer chemistry and polymer physics.

The properties of a polymer (mechanical, thermal, electrical, chemical to mention just a few) are directly governed by their molecular and supramolecular structure [7, 8]. By this we mean the shape of the molecule, and how the molecules act together as groups. The supramolecular structure can be further refined by distinguishing between its chemical and physical structure. Here the chemical structure pertains to the way the individual molecules are built, whereas the physical structure refers to the way the molecules arrange themselves.

The manufacturing process, where the polymerisation occurs (which is a chemical reaction) determines the chemical structure of polymers. During that process, the main valence bonds, or rather covalent bonds serve as connecting constituents between the bond partners. Molecular and supramolecular physical structure is the result of partial valence forces.

Both structures have a number of governing parameters assigned to them. For the chemical structure, these are:

² Velox, Bakelite

³ Polyamide 6, Polyamide 66

⁴ Kevlar



- The type and arrangement of the atomic chains
- The average molecular mass along with its distribution function
- The sequence length of the basic building blocks
- The number, distribution and length of the arborisations, i.e. the branching behaviour
- The type of substituents and end groups, i.e. what is being attached along the chains, apart from hydrogen atoms
- The sterical arrangement of the substituents, i.e. what is the three-dimensional layout of the above groups

Apart from the polymer molecules themselves, for the material to be fully chemically characterised, information about the kind and quantity of additives (e.g. fillers, softeners, stabilisers, lubricants and flame retardants) is necessary. The chemical structure will to the largest extent remain unchanged during mechanical processing. However, excessive thermal loading may damage the polymer, manifested by e.g. decomposition, depolymerisation and chain degradation.

The physical structure in a polymer contains (depending on the generic morphological form [9]) contains the amorphous state, the crystalline state and the mixing zone of the two states⁵. The crystalline state is considered to be that volumetric part of the plastic that contains a repetitively ordered structure of any form, whereas the amorphous state is that volumetric part which has no recognisable structure. The mixing zone is clearly the boundary layer between structured and unstructured domains. We would like to emphasize, that the crystalline state is not really a crystal, but likened to a crystal because it has repetitive substructures, which we dub crystallinity.

Key parameters governing the physical structure are:

- The state of orientation of the molecules/molecular groups
- The energy elastic residual stress
- The short range order
- The degree of cross-linking
- The degree of crystallinity and its distribution
- The size and distribution of spherulites, which is an observed crystalline substructure.

In essence, each macroscopic property of a plastic is governed by a different set of parameters; this prompts a selective influence of the physical structure on the properties. One particularly interesting and revealing structural parameter is the degree of crystallinity [10], from which the quality of the material processing can be deduced. The crystallinity distribution allows for the homogeneity of the structure to be assessed. Crystallinity directly influences the following properties (as an example): chemical durability, tribological fitness, thermal resilience, strength, transparency, ductility and toughness [11]. The relation between structure and property can be quantified using the following significant structural parameters [7]:

Amorphous	Crystalline
Orientation	Degree of crystallinity and the resulting supramolecular structure
Residual stress	Characteristic of the amorphous phase
Short range order	

Table 1: Significant structural parameters for amorphous and partially crystalline plastics.

As an example, the UTS for a mostly amorphous plastic is going to be influenced by the orientation, the residual stress and the short range order. If on the other hand, the plastic is mostly crystalline, that same property is going to be governed by the degree of crystallinity and its behaviour, and then to a lesser extent the behaviour in the amorphous phase we just discussed. The degree of crystallinity in a plastic is always limited, for example PA66 is between 35% and 45%. Whereas POM has a typical degree of crystallinity between 70% and 80%, as does HDPE.

We are going to consider in this article non-reinforced (partially) crystalline plastics. These contain multiple states or phases, with clearly identifiable geometrical substructures, which on a micro-scale level indicate a certain amount of deterministic structure. The following is simplified account of the formation of such entities (crystalline growth) in a quiescent melt. More detailed treatises can be found in [12-15].

⁵ Usually, the amorphous phase tends to be synonymous with entropy elasticity (rubber elasticity) and high ductility, whereas the crystalline phase is described by energy elasticity and high strength.



Beginning with a very small nucleus (typically around 25 nm diameter) and based on a bias of favourable growth direction with respect to energy, monomer units will begin to form macromolecules over time. It is interesting to note that each plastic displays its own critical weight, at which the growing chain will fold 180 degrees and then continue to grow. Fig. 2 depicts schematic macromolecular growth in a generic melt domain.

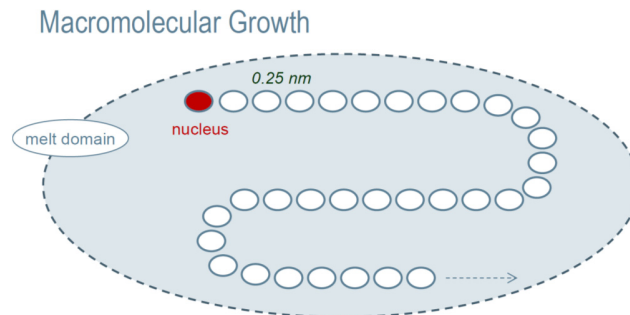


Figure 2: Macromolecular growth and chain folding in a generic melt domain.

As the chain continues to grow, the folding will occur at repeated positions and begin to form a lamellar structure. The eventually developed lamellae reach thicknesses between 20 to 60 nm. It is helpful to think of the chain as crystalline, and the remaining volume fraction as amorphous. At this stage we are not concerned with orientation effects or density gradients as a result of manufacturing, we simply think of the growth process from a general point of view. This structure creation is first present in the polymerization process⁶, and will be mostly carried over to the manufacturing process to be applied later. The manufacturing process itself will only influence the physical structure. Here the structures we have formed in the polymerization process can be realigned and reshaped as well as new ones formed. Fig. 3 shows the schematic growth of a single lamella in the melt.

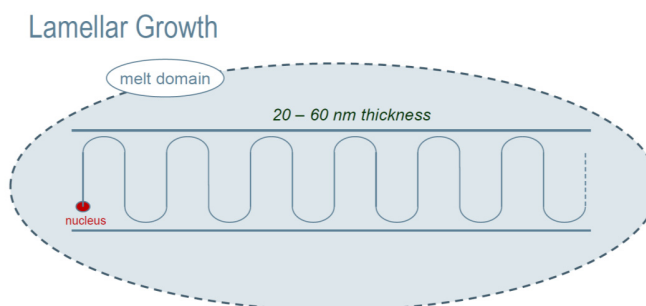


Figure 3: Lamellar growth as a result of extended macromolecular growth.

The length of the lamellae is finite, and determined mostly by a critical energy level, but also by geometric and structural boundaries. One such boundary is the fact that multiple lamellae begin to grow at different points in time and at different positions in the melt. However, from the nucleus mentioned in Fig. 2, multiple further lamellae will also grow in a radial fashion, such that a geometric structure often akin to a circle becomes apparent. Other possible shapes are maltese crosses, disks and “shish kebabs”, the latter being a stack of the previous geometric structures. The geometric structure arising from this radial growth pattern is dubbed a spherulite [9]. Fig. 4 shows a crossed polar examination of spherulite nucleation in a melt.

Though not strictly true, the growth is generally considered to be two-dimensional. The three-dimensional aspect is more being used for simulations of the degree of crystallinity [12-14, 17-22] and not necessarily describes the geometric shape of a structural entity. It is important to note that non-crystallized material exists between lamellae, adding a further layer of complexity to the constitutive behaviour. We refer to this volume as inter-lamellar.

⁶ Which is the manufacturing process of the plastic after which it is ground into pellets to be later remelted and formed into the final component shape.

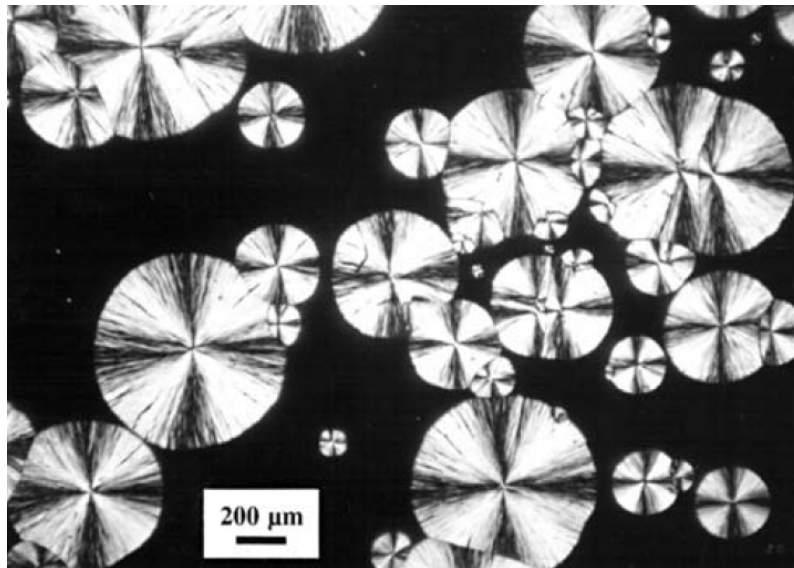


Figure 4: Spherulites of i-PolyPropylene growing from the melt, notice the spherical nature and Maltese crosses [16].

Introducing yet another simplification (referring back to Fig. 3), we will assume that the radial lamella growth is concurrent for each individual spherulite. Since the spherulites began to nucleate at different points in time, this in turn means that their boundaries will start colliding at certain locations in the melt. Areas between spherulites that have not crystallized, and where nucleation has ceased, are referred to as inter-spherulitical volume, which will to a major extent be amorphous in nature. These events are illustrated schematically in Fig. 4.

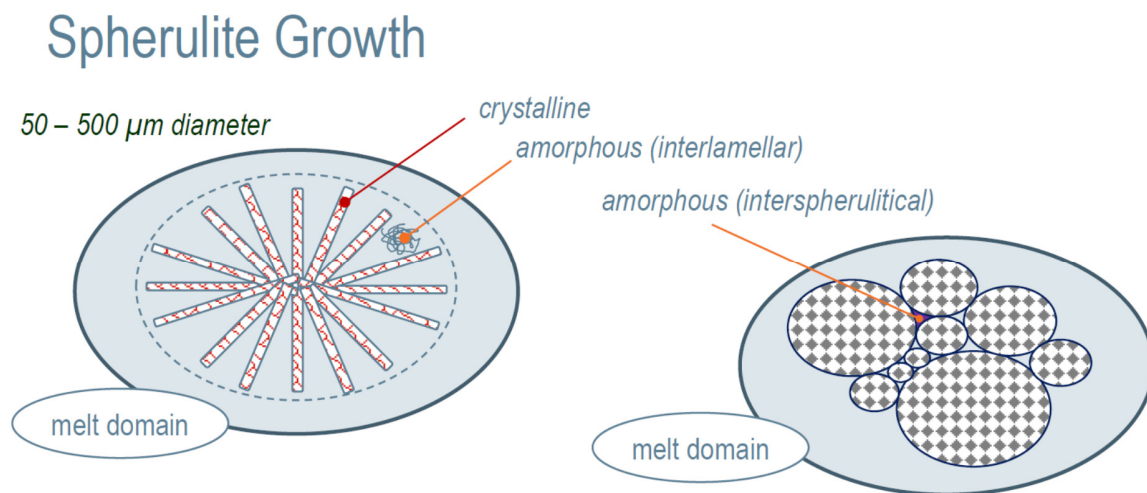


Figure 5: Spherulite growth and volumetric designation of amorphous and crystalline states.

On the whole, the crystalline volume fraction of the general melt domain is responsible for stiffness, strength, temperature performance and has a high density. (This explains the difference in behaviour between LDPE, having 45-55% crystallinity and HDPE having 70-80% crystallinity). The amorphous volume governs toughness, impact performance and damping, its density being lower than that of the crystalline volume.

As a closing piece to this section we have added a classical scale depiction of the structural entities discussed in the preceding paragraphs. It serves to illustrate the big picture in terms of morphological complexity for plastics, as well as indicate the level of detail necessary to capture in analytical or numerical assessment schemes.

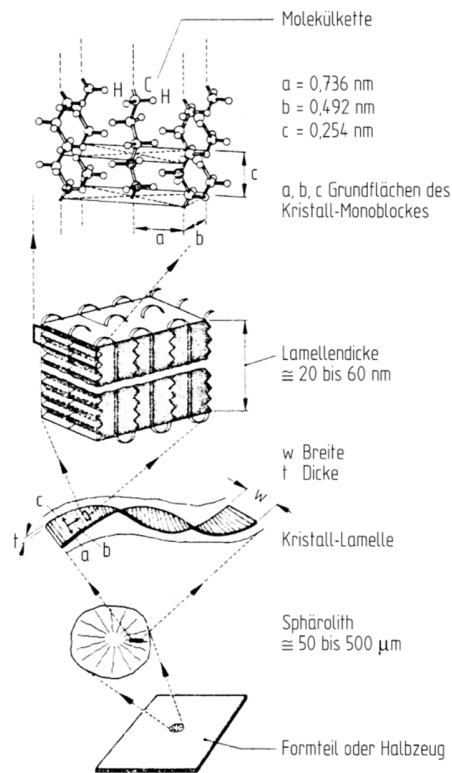


Figure 6: Composition of a partially crystalline structure for the example of PE [23].

CORRELATION BETWEEN STRUCTURE AND PROPERTIES

Having briefly reviewed the morphology of plastics, it becomes evident that concepts of integral mechanical properties, for a type of plastic do not apply. One can therefore not give an answer to the question “what is the isotropic Young’s modulus of PE” directly. Instead, it becomes necessary to think about plastics as multi-component materials on a constitutive level. This is the reason for which nonlinear, multilayer, multi-scale material models have proven to be much more successful at numerically reproducing force-deformation behaviour on a time scale from actual physical tests than conventional material models. The dependency of mechanical properties of plastics on its chemical and physical structure has been investigated, recorded and confirmed by various authors, see e.g. [7, 10, 24-26].

In order to visually quantify the correlation between structure and property, three distinctive diagrams are presented. The first (see Fig. 7) depicts the dependency of the UTS for PS (Polystyrene) on the orientation. The data was recorded for different densities and energy elastic residual stresses. At high degrees of orientation, it is possible to achieve a near 100% increase of the UTS.

The second diagram (see Fig. 8) depicts the secant modulus for injection moulded PP as a function of the surface layer thickness fraction. The surface layer thickness is influenced by the injection moulding process. A large increase in the measured quantity can be observed with increasing surface layer thickness, which in turn can be traced back to high molecular orientation in the surface layer.

The third and final diagram (see Fig. 1) shows the UTS as a function of the density for PS, this time for fixed degrees of orientation and no residual stress in the test specimens. In contrast to Fig. 6, an optimum combination of orientation and density can be observed, after which there is no apparent further increase to be gained.

At this stage we can conclude that regardless of amorphous or partially crystalline states, the morphology directly influences the properties and thus needs to be accounted for in any form of investigation, phenomenological, analytical or numerical.

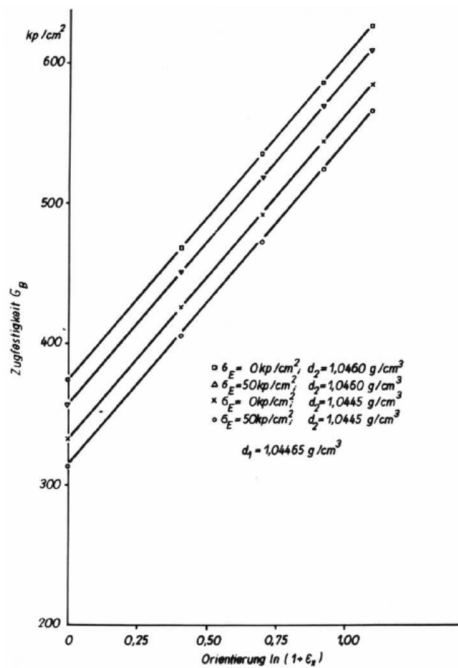


Figure 7: UTS as a function of orientation for PS. [7]

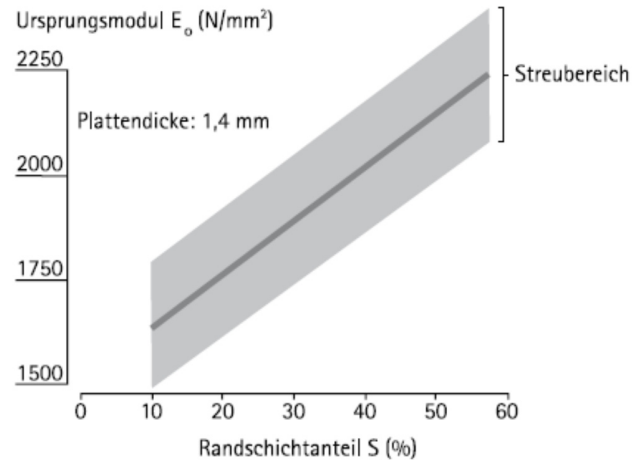


Figure 8: Secant modulus as a function of surface layer for PP. [25]

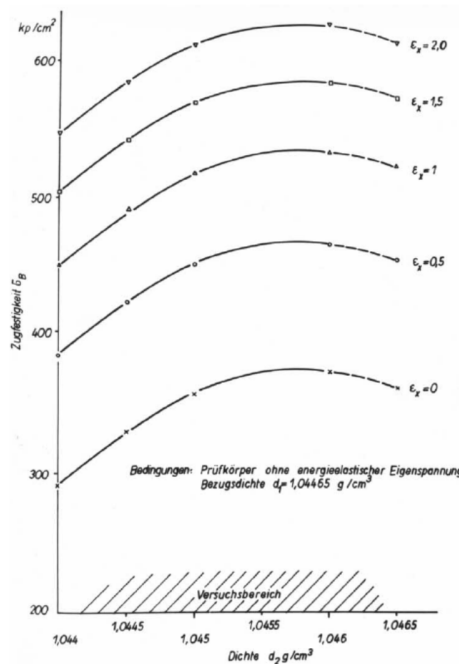


Figure 9: UTS as a function of orientation for PS. [7]

THE ROLE OF THE MANUFACTURING PROCESS SKIN

Injection moulding is by far the most widely used manufacturing process for large quantities of engineering components. Extrusion and die casting are also used, but to lesser extents. One of the main features of injection moulding and casting that the non-isothermal cooling of the melt causes the layer closest to the mould to freeze much quicker than the rest of the bulk. Apart from causing density gradients to evolve through the wall thickness, strong orientation of the surface layer (or skin) will result where a melt (or near melt) is being pressed into a specific shape. This is the case for injection moulding and extrusion. The highly oriented skin has much higher ductility, stiffness and strength than the interior of the component [27]. This characteristic creates a beneficial protection, in that the skin acts as a



wrapping foil, which for a long time prevents initiated cracks from breaking to the surface. Indeed, unless a surface has been mechanically compromised, it is extremely unlikely that a crack will initiate anywhere else than from within the bulk [28, 29]. The crack growth behaviour will be discussed further in the subsection “Experimental observations”.

THE FATIGUE BEHAVIOUR OF NON-REINFORCED PLASTICS

In order to address the fatigue behaviour of plastics, we need to briefly and critically review established ideas for metals. The value of this review is to provide an objective reference frame from which a physically justified description for plastics may be derived.

Stress-based fatigue strength assessment (SN):

This is the oldest fatigue analysis philosophy. It relies heavily on engineering experience and empirical factors, and becomes increasingly complex as nonlinearities are added. In essence it utilizes two concepts;

- Assessment of the fatigue strength using nominal stresses
- Assessment of the fatigue strength using local stresses

Stress-based fatigue is still the basic starting point for most design calculations. It has a vast experience-based user database to fall back on, although this database is spread on individuals and organizations and not collated in any form. The FKM guide line [30] however, constitutes an exception to the above. SN analysis generally requires the use of quite a few correction factors, and new findings are often incorporated through yet additional factors. The large number of factors makes the approach potentially error-prone. Another source of controversy is the way SN data is reported. It is usually provided in the manner of life as a function of nominal stress. It is oftentimes unclear whether push-pull, rotating bending, flexural bending or torsion was used, and the specimen dimensions are generally not presented. SN-based fatigue algorithms are constantly being extended/improved/corrected to account for shortcomings in the basic assumptions and the lack of real material representation in the fatigue calculations. Users with application-based experience are usually in a position to obtain high quality result, regardless of the algorithm or method applied. The continuous transfer of this knowledge is one of the weak points of SN analysis.

Strain-based fatigue strength assessment (eN):

Strain-based fatigue is a comprehensive approach that can treat both high-cycle (HCF) and low-cycle (LCF) fatigue⁷. The basic principle is that fatigue cracks nucleate from localized plastic straining (deformation). It uses the concept of cyclically stable material data, and assumes that changes in cyclic behaviour are more pronounced in the early stages of loading. A further tool utilized is the Ramberg-Osgood relationship to describe the material behaviour for many metals. Life is depicted using the Coffin-Manson curve, which expresses the sustainable number of cycles applied as a function of strain amplitude, where the amplitude is resolved into elastic and plastic components. Strain-based fatigue assumes that fatigue in the HCF region is more dependent on strength, (essentially SN thinking) and in the LCF region on ductility. One important assumption utilized is that crack initiation occupies most of a component's fatigue life. The cyclically stable material data required by strain-based fatigue algorithms can be determined through uniaxial testing and are more readily available than stress-life data. A further useful technique deployed, is the incorporation of mean stress effects directly into the strain-life equations. Although a physically more accurate description than SN analysis, the simplification of the elastic plastic behaviour into a Ramberg-Osgood law, and the still overt dependence on linear elastic FEA with non-bullet proof plasticity corrections make the methodology less accurate than it could be.

Fracture mechanics-based fatigue strength assessment (Paris/critical distance):

With fatigue life predictions involving fracture mechanics, we will allow for a crack to exist. This is different than the previous two algorithms, where either it is assumed that there is full fracture or just initiation. The question we can then ask is whether the crack propagates, and if it does how much life do we gain without compromising structural integrity and performance of the component.

⁷ Here we mean by HCF, component failure exhibited at more than 10^6 cycles and LCF between 10^3 and 10^5 cycles, otherwise crack propagation becomes the dominant contribution to actual component survival.

Fracture mechanics is a relatively new engineering tool for life assessment. The discipline provides a quantitative understanding of the reduced strength of a component in the presence of flaws or cracks. In essence it attempts to cover all three regions of the "fatigue life", these being:

- Crack initiation
 - Micro-cracks form macro-cracks
- Stable crack propagation
 - Possible to describe using a Paris law
- Unstable crack growth and ultimate fracture
 - Usually 1 more cycle, at criticality, so could be ignored in a fatigue estimate.

These concepts are already being employed in the aerospace industry, where cracks are omnipresent, but airplanes still fly with them. Simply using an SN or eN analysis to get to the point of initiation would be overly conservative and costly. Rather, structures need to be fault tolerant, and it is estimated whether a crack will extend in a stable fashion during the period between inspection intervals. If so, the component is kept in service.

The theory of critical distances [31, 32] is a first foray into this area, where one allows for cracks, but tries to make an estimate whether or not they will ever propagate to fracture. Here a comparison is implicitly made to the available energy release rate in the stressed component to the critical fracture energy. If this factor is sufficiently low, we are typically below the threshold part of the Paris law, and the crack will not propagate. The critical distance is essentially the length scale which is being used to convert energy densities into fracture energies, which makes it a material parameter.

One of the benefits of fracture mechanics is that it allows for thorough understanding and study of a broad range of fatigue crack growth mechanisms. Crack growth life is sensitive to the initial crack size, because it changes the stress distribution through the component. From a practical point of view, it is vital to minimize initial crack or discontinuity size, something which in turn places further requirements on manufacturing processes regarding cleanliness.

Fracture mechanics is a constantly evolving field, which continues to improve, and is the focus of a very active research community. There are of course limitations regarding the applicability of fracture mechanics; linear elastic fracture mechanics is limited to cracks in brittle materials. These limitations can be partially overcome by using elasto-plastic fracture mechanics, which assumes a different form of the singularity at the crack tip. For either, the idea is to correlate the crack propagation rate with the elastic-plastic deformation around the crack tip (J-integral, $\Delta CTOD$ and yield-strip approaches). Anisotropic material properties can be taken into account using microstructural fracture mechanics (MFM). In spite of the limitations mentioned, a reasonable correlation between theory and experiment can be found. Typically, it is still required that the fracture process zone is contained in a sufficiently small annulus around the crack tip, and otherwise one might get interactions with other processes in the material.

Multiaxiality:

Rather than going into a lengthy discussion on the nature of multiaxial stress states in plastic components, we are going to content ourselves with pointing out that even in a uniaxial load case, the presumption of a uniaxial stress state does not hold true. This can easily be explained by the transverse contraction of a bar or rod due to Poisson's effect, or by the analogy of a double-sided fillet in a plate subjected to a uniaxial load, which is clearly biaxial, see Fig. 10.

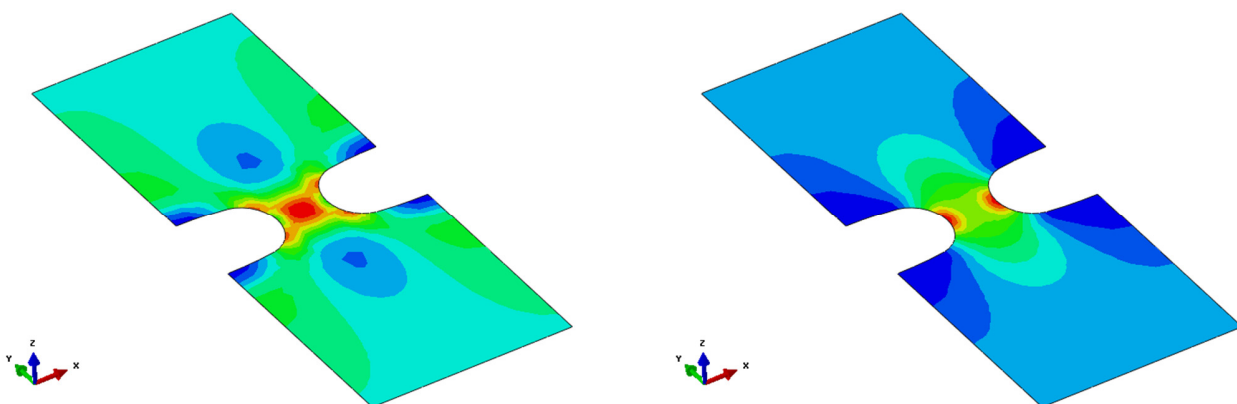


Figure 10. Uniaxial loading of a plate with double-sided notches. σ_{xx} left and σ_{yy} right.



The biaxiality ratio defined as σ_{yy}/σ_{xx} yields a value of 0.42 for a linear elastic load case. Biaxiality affects the type and severity of fatigue damage, it is effectively an indicator in which direction a crack will form. Typically one assumes that the direction is such, that when we resolve the stress intensity factors on that plane, that $K_{II} = 0$.

A “real world” plastic component will for the most part experience a triaxial stress state in the vicinity of critical design elements⁸. Fig. 11 shows a schematic representation in a Cartesian coordinate system.

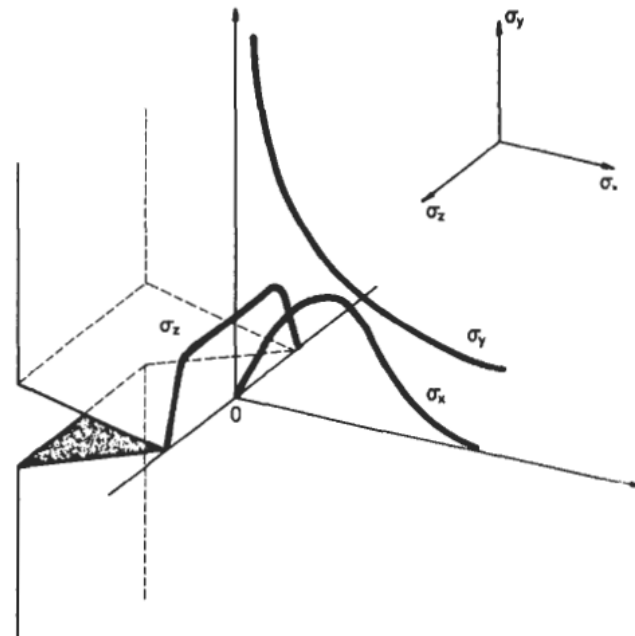


Figure 11. Triaxial stress distribution in a crack [Crawford].

The stress triaxiality has been used by Kanvinde & Deierlein [33-35] as an index to track increase and decrease in the volume of voids as a means of predicting low and ultra-low cycle fatigue of structural steels. This concept is referred to as the cyclic void growth model (CVGM). Experimental validation by Cravero et. al [36] further emphasizes the importance of incorporating the triaxial stress state into fatigue life predictions.

Recalling the morphology of plastics in a three-dimensional body, we postulate the following:

- Based on the geometrical restrictions, nucleation characteristics and maximum possible crystallinity, a unit volume of plastic consists of a mixture of discs, small spheres, shish-kebabs and Maltese crosses. These are surrounded by apparent entropy elastic material (the amorphous fraction) and held together by a strongly oriented high strength elastic wrapping foil.
- The entities mentioned can all be categorized as flaws, each of which possesses individual apparent fracture energy. This fracture energy governs the direction that an initiated crack will take throughout the unit volume.
- The most likely place for a crack to initiate in an injection moulded, extruded or die cast plastic component is from within the bulk of the material unless the protective skin has been mechanically compromised.

The postulates allow us to simplify the view on multi-axiality and treat it from an entirely energy-based point of view.

One additional mechanism that is dependent on the degree of multi-axiality of the stress field is the growth rate of crazes. Crazes are (in a grossly generalized manner) cracks that form as a result of microvoids, which while expanding are held together by fibrillar bridges. Once the fibrillar bridges break, a macroscopic crack has formed.

The topic has been treated in great detail by researchers such as Michler [37] and Kausch [38,39]. Examples of a crazes are shown in Fig. 12 and Fig. 13. Interestingly enough, crazes, being formed through voids, are unaffected by the morphology and always grow perpendicular to the direction of the applied load.

⁸ E.g. fillets, inserts, bosses, rib junctions, bolt holes

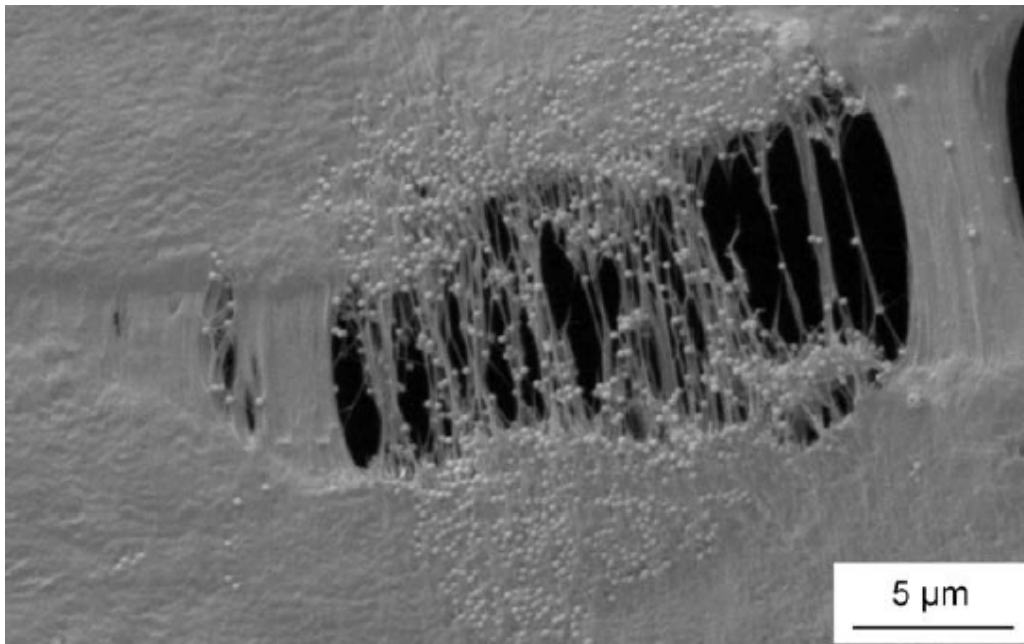


Figure 12: A single craze in PE [40].

Fig. 12 shows an ESEM⁹ micrograph of a craze in PE, subject to a load in the vertical direction. The rupturing fibrillar bridges are clearly visible.

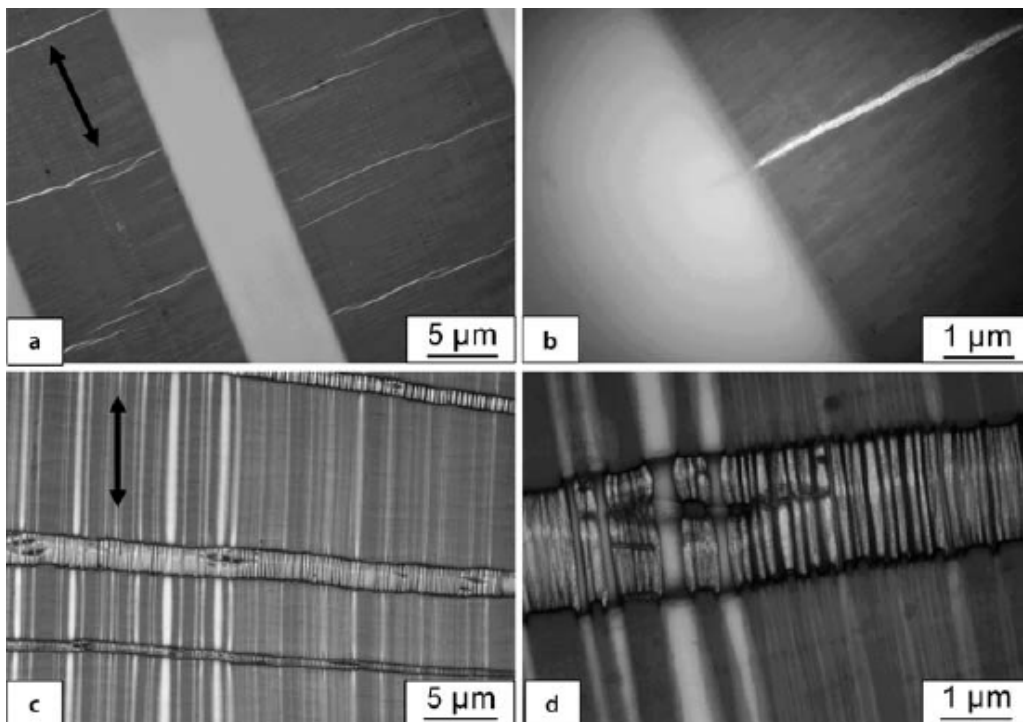


Figure 13: Crazes in PS/PMMA [40].

Fig. 13 shows HVEM¹⁰ micrographs of multiple crazes in PS/PMMA. The load direction is indicated by the black arrow in images a and c.

⁹ Environmental scanning electron microscope



Experimental observations

Beginning with the morphological aspects, the following observations are of vital importance:

When considering a crystalline polymer structure, cracks which have the potential to propagate may initiate as a result of molecular slip. There are also findings that pinpoint the spherulite boundaries as weak areas where cracks can develop following excessive straining. The boundaries may of course also serve as the path of crack propagation.

Amorphous structures tend to exhibit cracks developing in voids that form as a result of viscous flow.

Crack initiation sites can also manifest in the form of moulding defects¹¹ (see Fig. 14, Fig. 15 and Fig. 16), filler particles¹² and geometrical discontinuities.



Figure 14. Weld line in a plastic component. [41]

¹⁰ High voltage electron microscopy

¹¹ Weld lines, gates, voids, density discontinuities

¹² Pigments, stabilisers, flame retardants, lubricants



Figure 15. Void and inhomogeneous melt in a plastic component.[41]

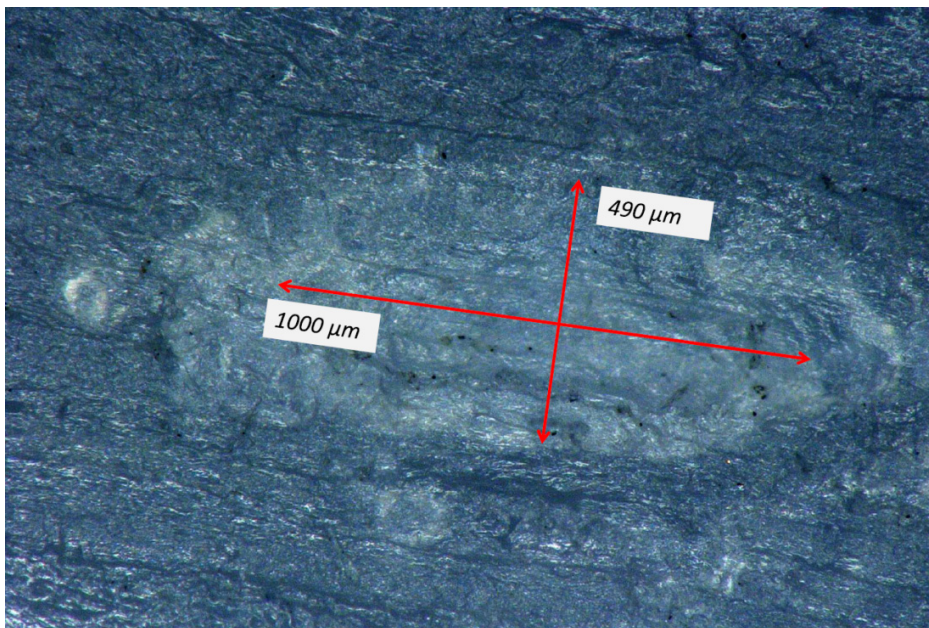


Figure 16. Density discontinuity in a plastic component.

We will close this section with a few key experimental observations that speak a clear language regarding the damage behaviour and origins of non-reinforced plastics. The first observation (see Fig. 17) is a microtome cut showing the morphology of an injection moulded DIN EN ISO 3167 type A specimen made of PA66. Larger Maltese cross-shaped spherulites dominate the bulk of the structure, their size decreasing with the distance to the surface. The highly oriented skin is also clearly visible, along with the so called trans-crystalline region between the crystallized bulk and the surface layer.

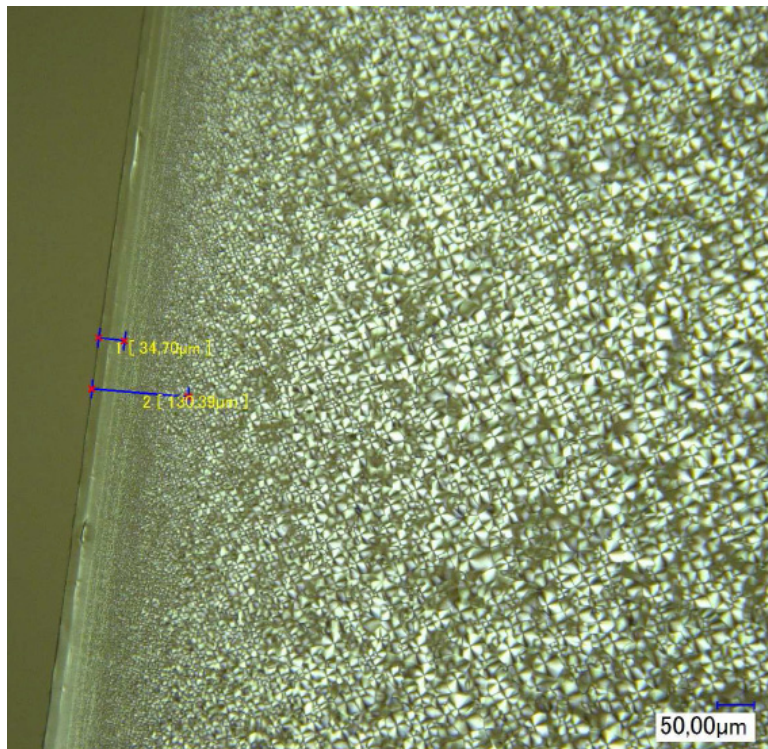


Figure 17. Typical morphology of injection moulded PA66.

Fig. 18 shows a microtome cut from a specimen made of POM. The difference in morphology is distinct, in that the spherulites are slightly elongated and that the injection moulding skin is much thicker (roughly 3 times).

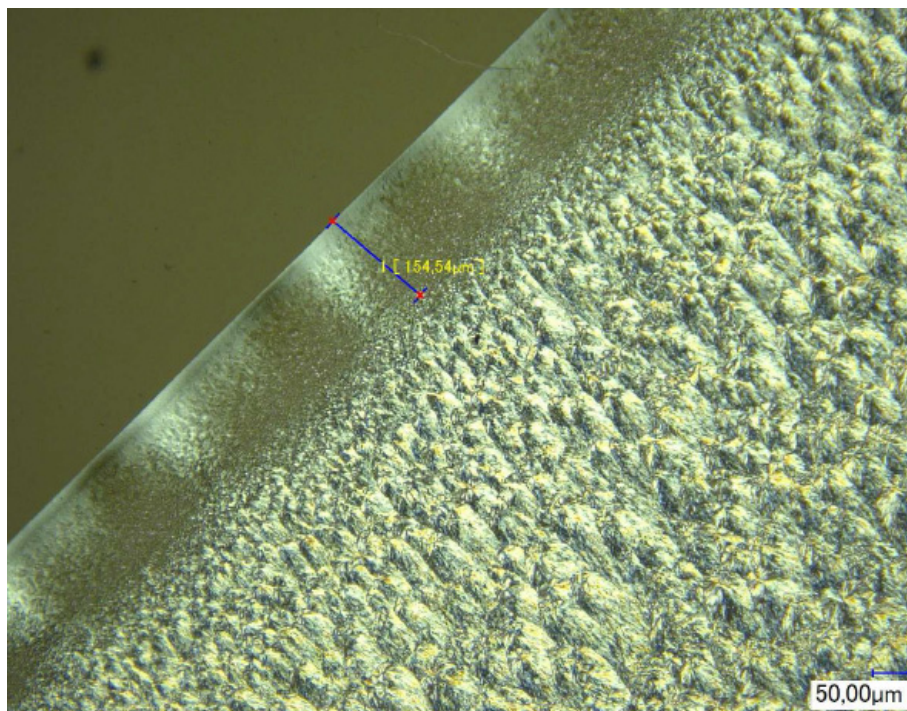


Figure 18. Typical morphology of injection moulded POM



Fig. 19 is a micrograph of the fracture surface on a specimen made of POM tested in uniaxial fatigue. The damage initiation and the subsequently forming voids in the centre portion are clearly visible (the little black spots), the distance between beach marks growing larger and larger as the fatigue process progresses radially outward.

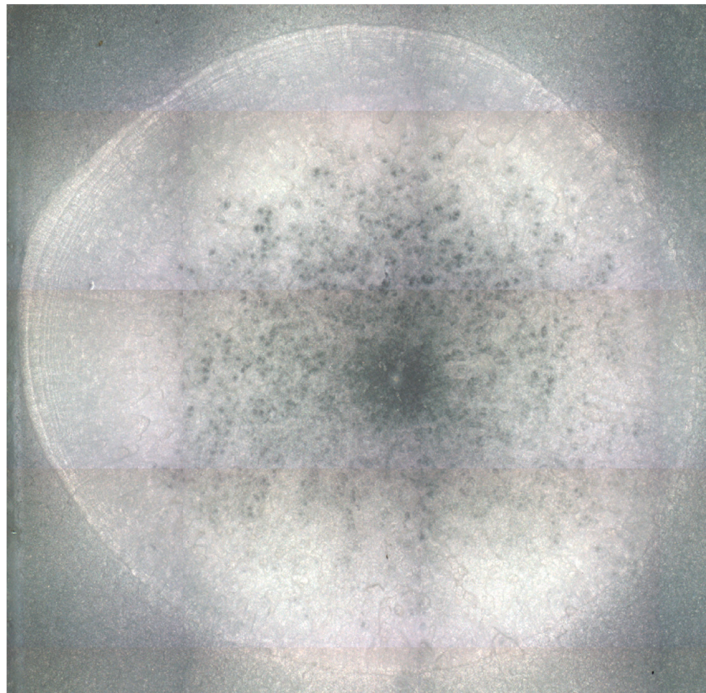


Figure 19. Fatigue fracture in a POM tensile specimen.

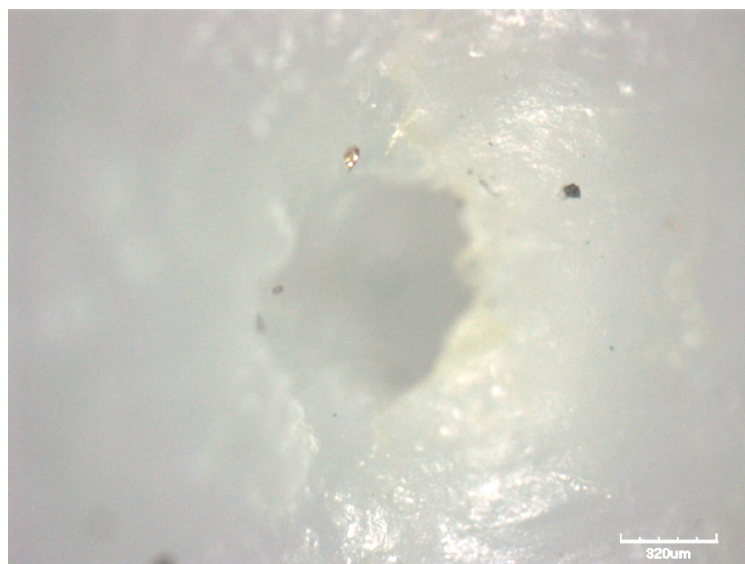


Figure 20. Void in the bulk of a plastic component as a result of cyclic loading.

Fig. 20 shows a void inside the bulk of a component subjected to cyclic loading. The initial morphology was homogenous with no voids present after the manufacturing process. The void was detected after complete rupture of the component in a duty cycle test.

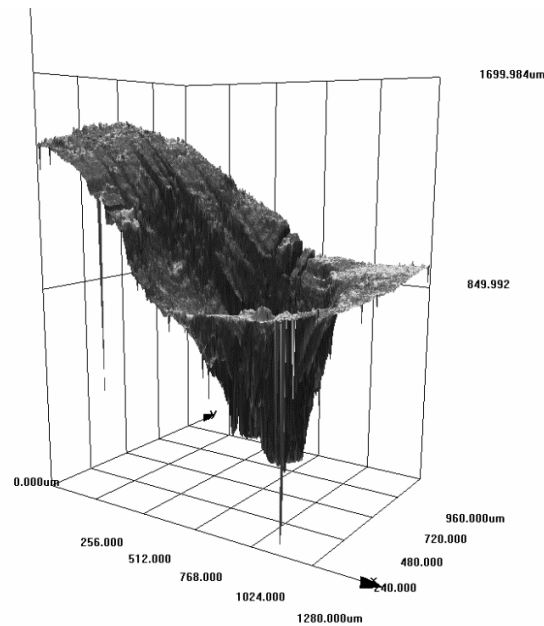


Figure 21. Three-dimensional scan of the void in Fig. 14.

Fig. 21 shows a three-dimensional scan of the void geometry with units in micrometres. The severity of the void as a stress raiser and its manifestation in the form of reduced structural integrity is evident.

The previous section serves to visualize the morphological complexity of plastics, and how this directly governs properties and structural performance. Particularly with respect to fatigue, it is clear that any uniaxial approach to fatigue life prediction applied will meet with limited success.

The role of the manufacturing process skin also becomes more tangible and with it, the explanation for bulk initiating fatigue cracks increasingly obvious, especially from a polymer physics point of view.

TEMPERATURE

A part from morphological differences with the way in which fatigue presents itself in plastics as compared to metals, a further significant differentiator with respect to classical materials is temperature. The difference stems from the fact that plastics are poor conductors, while at the same time, they dissipate a relatively large amount of deformation energy into heat. In other words, self-heating becomes an issue. The key behaviour is yet again related to the morphology. Plastics consist of long chained molecules that are strongly intertwined. Applying a deformation to the material will typically incur two distinct responses.

Firstly, there exists some quantity of reversible energy storage in the material, which is comparable to the straightening of a coiled spring. This is morphologically equivalent to the stretching of the chains. The reversible energy storage mechanism is on a macroscopic scale interpreted as elasticity, but since the internal structure changes as a result of the deformation, the elastic behaviour is hardly ever linear.

Secondly, irreversible energy is being dissipated as a result of the long chains sliding along one another. This is typically internal frictional behaviour, which is comparable to plasticity. However, in plastics this frictional behaviour is strongly rate dependent, and thus on a macroscopic scale we can interpret this behaviour as viscosity. The internal mechanisms acting here are complex, and the behaviour can be construed to be anywhere in between viscoelastic and viscoplastic.

Let us clarify the terms in our interpretation, because there are often subject to inconsistent use. We term the behaviour viscoelastic when the material returns to its original state over an arbitrarily long period of time when we remove the load. If the material it does not return to its original state, we call the behaviour viscoplastic.

The standard way of modelling of plastics in numerical analysis is often performed with the assumption of viscoelasticity, but the actual behaviour is a non-trivial combination of both viscoelasticity and viscoplasticity. The chains will be somewhat locked in place while being pulled alongside other chains, but at the same time no real anchor exists. So after

applying a load for a sufficient amount of time, irreversible changes occur in the micro structure. It is our contention that the accumulation of small amounts of viscoplastic deformation is the primary cause of fatigue of plastics.

After discussing all the morphological issues in play, we note that there is indeed a relatively large amount of energy dissipation occurring in plastics under fatigue loading which does not diffuse away as quickly as it could in metals. The local dissipation causes local heating, which in essence simply constitutes local vibrations of the molecules. The increased vibrations enable the internal structure to gain access to relatively more space, and thus the sliding behaviour of the chains becomes easier. This is from a macroscopic viewpoint perceived as a reduction in the effective viscosity at an increased temperature. Lower effective viscosities have lower dissipation rates, which causes the local temperature rise to slow down with increasing temperature. To visualise the effect of viscosity on the behaviour of the material we will next conduct an exemplary analysis on a purposely simplified plastic material.

A (generalized) Maxwell model of a plastic

The overall behaviour discussed up to this point can be strongly simplified into a Maxwell model [6] as illustrated in Fig. 11.

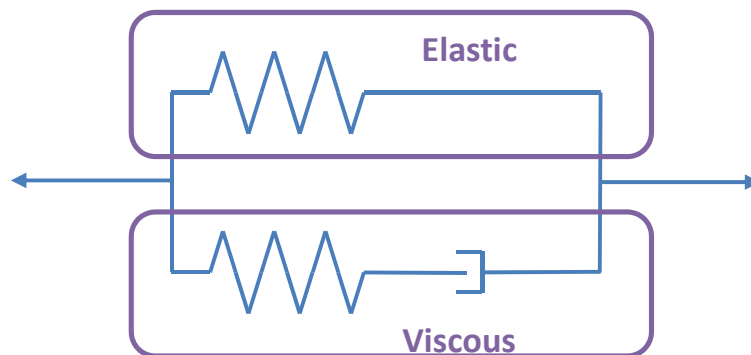


Figure 22. Simplified idealised behaviour of a plastic as a Maxwell model

In this figure we have simplified the behaviour of the plastic so far as to assume that it is viscoelastic. We generalize immediately though into stating that neither of the springs as shown in the network would need to be linear, and that the damper is not linear by any means. We should be content by noting that there is a damper. We have also omitted the viscoplastic part of the behaviour which we assume is responsible for the fatigue behaviour.

With that in mind, let us perform a quick analysis of what happens when we *do* assume linearity, and merely introduce temperature dependence. This is to address the additional complexity that arises when dealing with a temperature dependent plastic.

Also, for sake of argument to understand the mechanics, we are going to assume uniaxial behaviour. Thus, given the Maxwell model as in Fig. 22, we will call the upper part of the network the elastic layer, and the lower part of the network the viscous layer.

We now have some balance equations that need to be satisfied:

1. The strain as observed by the elastic layer and the viscous layer are the same, it is the total strain over the network.
2. The stress over the network is equal to the stress of the elastic layer plus the stress of the viscous layer.
3. The stress in the spring in the viscous layer is equal to the stress in the damper in the viscous layer, they are in equilibrium.
4. The strain in the spring in the viscous layer plus the strain in the damper is equal to the total strain over the network.

Let us now introduce some terminology to put these observations into equations. The stiffness of the upper spring is given as E_0 , the stiffness of the lower spring is given as E_1 and the viscosity of the damper is given by η . Also denote by ϵ the total strain applied over the network and ϵ_e the strain in the spring that goes into the viscous layer and ϵ_v the strain that goes into the damper in the viscous layer. Finally, let us call the stress in the elastic layer σ_0 and refer to the stress in the viscous layer as σ_1 . The total stress over the network is given as σ .



The first together with the fourth condition gives us $\varepsilon = \varepsilon_e + \varepsilon_v$. The second condition yields $\sigma = \sigma_0 + \sigma_1$, where $\sigma_0 = E_0 \varepsilon$. Finally, the third conditions gives us $\sigma_1 = E_1 \varepsilon_e = \eta \dot{\varepsilon}_v$. Here the dot above the viscous strain refers to the rate of the viscous strain.

We now assume that we are going to subject the network to an oscillating load $\sigma = \sigma_a \sin \omega t$. We can now rearrange all the equations to give us an ordinary differential equation to solve:

$$(E_0 + E_1) \dot{\varepsilon}_v = E_1 \sigma_a \sin \omega t - E_0 E_1 \varepsilon_v$$

We solve this equation to find the strain at a given frequency. The result is that our strain will be described accordingly

$$\varepsilon = \sigma_a (C_1(\omega) \sin \omega t + C_2(\omega) \cos \omega t)$$

Here $C_1(\omega)$ and $C_2(\omega)$ are the in and out of phase compliance.

The above allows us at this stage to deduce some interesting behaviour. First note that when $\omega = 0$, the out of phase compliance is 0, thus we see pure in phase behaviour. The in phase compliance then simplifies to $1/E_0$. A rotational frequency of 0 essentially means that we are performing the oscillations extremely slowly, and we will only see static behaviour. Looking at our network we can observe, that if the damper is given sufficient time to relax, the only stress arising will be that of the elastic layer.

For the case of $\omega \rightarrow \infty$, the out of phase compliance is again 0, as the denominator will dominate the numerator for large values of ω . Conversely, the in phase compliance will drop to $1/(E_0 + E_1)$, since essentially the fraction involving ω in our result will slowly approach 1. This is in accordance with what we would expect. An infinite rotational frequency means that we are pulling on the network so fast, that the damper does not have time to relax, essentially rendering it infinitely stiff. This means that we are applying the load in the viscous layer to the spring only. The result is the observation of a stiffness which is the sum of the stiffness in the elastic layer and the viscous layer, which is $E_0 + E_1$. The in phase compliance is then merely the inverse of that as given previously.

Heat generated from the Simplified Model

Let us now direct our attention the matter of interest, which is the temperature effect. As we already stated, the temperature rise is caused by the dissipation of energy. Let us therefore study how much energy is dissipated per unit time over a single cycle of the load. We can express this rather simply as

$$J = \frac{1}{T} \int_0^T \sigma \cdot \dot{\varepsilon} dt$$

Where $T = 2\pi / \omega$. We then find that

$$J = \frac{\sigma_a^2}{4} \frac{\omega E_1^2 \eta}{\omega^2 (E_0 + E_1) \eta^2 + E_0^2 E_1^2}$$

Which is caused by the out of phase motion. It should now be recognisable that a viscous material such as a plastic has quite severe amounts of dissipation. We can also see that every doubling of the stress amplitude at a given frequency quadruples the amount of energy being dissipated when the viscosity would remain constant. Let us now look at the one-dimensional energy balance equation [42]. This reads

$$\rho c_p \frac{d\theta}{dt} = -\frac{dq}{dx} + r$$

In this equation θ is the temperature, q is the heat flux (that is the amount of heat transported per second over a given area), r is a heat generating source term and ρ and c_p are the density and specific heat as usual. In order to come up with a representable solution we need to simplify this equation substantially even though we are already operating in the uniaxial domain. The heat flux is typically given through the Fourier law, but that would present us with a non-local problem, which does not have a trivial solution. We should bear this in mind, as it is one of the issues that will come back to haunt us when we want to perform physically realistic analyses pertaining to fatigue of plastics.



Let us assume, for the sake of argument, that we have a material point of interest, directly connected to the outside world with a film condition. In this case we take $dq/dx = k(\theta - \theta_a)$, where θ_a is the ambient temperature and k the effective conductivity in Watts per cubic meter per Kelvin. Thus, the amount of heat removed is simply a linear function of the temperature difference between the material point and some arbitrary environment. In reality this is extremely difficult to justify, since the correct heat flux will be a function of the geometry and the actual heat removed from the *specimen*, and not the material point, and it is a complex function of environmental conditions.

As for the heat generation term, this is the energy dissipation J which we already computed. To see whether we reach an equilibrium condition in terms of temperature or not, we need to set the rate of temperature change to 0, which yields

$$0 = -k(\theta - \theta_a) + \frac{\sigma_a^2}{4} \frac{\omega E_1^2 \eta}{\omega^2 (E_0 + E_1) \eta^2 + E_0^2 E_1^2}$$

Applying a further simplification (we just can't seem to stop ourselves), we assume that only μ is a function of temperature, and that the elasticity will remain the same. This is of course not the case, as the stiffness will typically also drop as the temperature rises. At this point we need to introduce the temperature dependence of the viscosity. Common choices for doing so are the Arrhenius model or the Williams-Landel-Ferry (WLF) model [43]. The Arrhenius model tells us that when the viscosity is dominated by molecular kinetics that

$$\eta = \eta_0 \exp\left(\frac{Q}{R\theta}\right)$$

In this equation, Q is the activation energy and R is the gas constant. The value η_0 is a reference viscosity. The Arrhenius model is essentially the same as the Reynolds exponential model. The WLF model is more suitable for polymer melts, and would therefore be our primary choice. In this case we have

$$\eta = \eta_0 \exp\left(-\frac{A_1(\theta - \theta_0)}{A_2 + \theta - \theta_0}\right)$$

Where θ_0 is a reference temperature and A_1 and A_2 are constants. Trying to solve these equations analytically is not possible for either Arrhenius or the WLF form. We will thus have to resort to a numerical scheme to give us a feeling for the numbers. Note that this is a numerical scheme applied to an already simplified problem. The numerical approach would become much more involved if we were dealing with all the actual (multi-axial) behaviours.

WLF Parameters	C_1 [-]	C_2 [C]	θ_0 [C]
	1	51.6	-15
Stiffness Properties	E_0 [MPa]	E_1 [MPa]	η [MPa s]
	7150	2285	4100
Heat Properties	ρ [kg m ⁻³]	c_p [J kg ⁻¹ K ⁻¹]	k [W m ⁻¹]
	1400	3000	126
Load Settings	θ_a	σ_a	f
	23	50	1

Table 2: Properties for the equivalent uniaxial calculation.

We will now invoke some numbers. Base properties are listed in Tab. 2. We are going to modify the loading settings to observe the influence pertaining to the temperature over time. The simplified analyses are going to take into account the dissipation, change of viscosity as a function of temperature, and convection of heat to the environment.

Applying the simple model at this stage, together with the heat equation, we can observe the behaviour as given in Fig. 23 and Fig. 24. Reviewing the figures, it becomes evident that the rise in temperature is strongly dependent on the frequency with which the load is being applied. We note that for this simple model, even at 1Hz, we see a distinct change in



temperature. Our intermediate conclusion is that accelerated testing of plastics will be very hard to conduct and to justify. The strong load amplitude dependence is also clear and present.

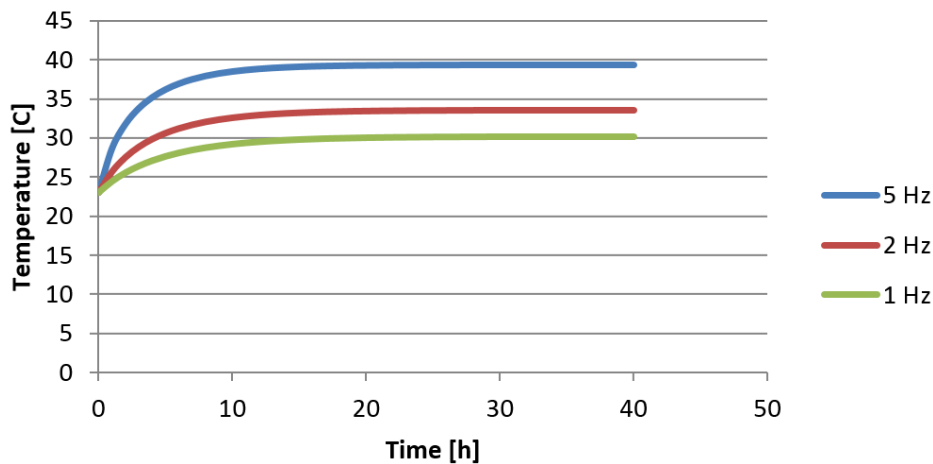


Figure 23: Temperature change as a function of frequency, all other properties constant.

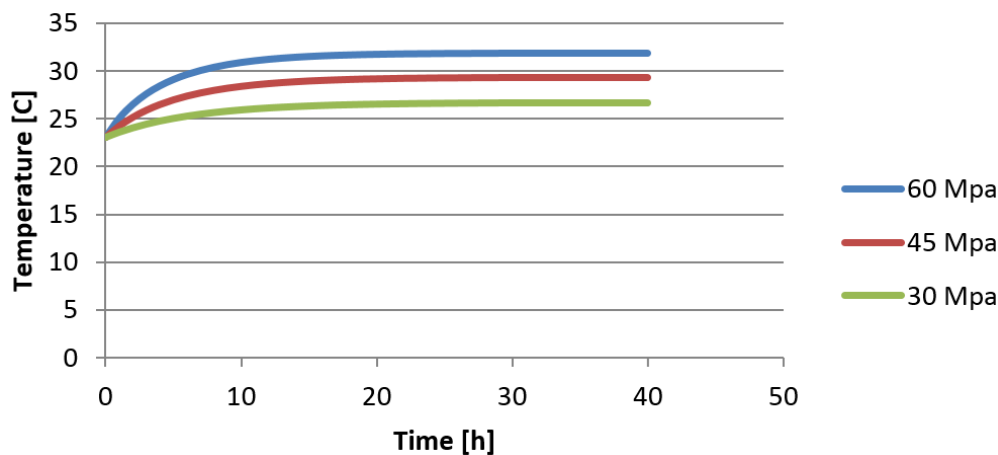


Figure 24: Temperature change as a function of load, all other properties constant.

The dependencies illustrated were based on strongly simplified behavioural laws, we assumed linear elasticity, one single elasticity layer, and linear viscoelasticity. Changing any of these assumptions is going to change the behaviour, either making the temperature change larger or smaller. What is also of critical importance is how the temperature is diffused into the remainder of the part, and convected to the environment. Depending on this behaviour we will see changing temperature behaviour at a material point.

Summarizing our findings, we can distinguish three load application speeds:

1. The load is applied very slowly. Energy dissipation occurs, but there is sufficient time for the heat to diffuse through the whole part. This means that we may consider the problem as isothermal. We note that this requires very low frequency loading. This case would produce the longest fatigue life.
2. The load is applied at a moderate speed. We can observe a higher rate of energy dissipation, but also insufficient time for all the heat to diffuse away. Thus, the local temperature rises. The temperature rise in turn lowers the viscosity, as well as the effective stiffness. This shortens the life of the part significantly, since the viscoplastic effects become more dominant and as such cause more internal damage.
3. The load is applied at a high speed. The result is a high rate of energy dissipation, and because there is no time for the heat to diffuse away, the process becomes adiabatic. We observe a rapid rise in temperature, and will typically see low cycle fatigue failure.

From the summary we can draw a set of conclusions:



- The fatigue life of plastics is strongly temperature dependent. This is because the primary cause of failure is ‘pull-out’ of the intertwined molecules. This process is facilitated by an increased temperature, since the pull-out resistance reduces significantly.
- Plastics have relatively high dissipation rates, which are themselves strongly temperature dependent due to changes in viscosity. This fact causes isothermal measurements of fatigue life to be more complicated than for metals.
- Due to the severe temperature dependency of plastics, fatigue life analysis needs to take this into account. This will cause additional analysis costs, because:
 - We need to compute a temperature distribution, which is related to the magnitude and speed of loading. The computation of such a temperature distribution means that simply using a single linear analysis with a stress correction, one way or another, will be insufficient.
 - Further, not only will the FEA analysis need to be more involved, but the fatigue calculation will also need to become more complex. Merely using the highest temperature arising from the computed temperature distribution will yield strongly conservative results, and thus the temperature changes need to be taken into account in a fatigue calculation.

AN IDEAL ANALYSIS WORLD

The following section is concerned with outlining what we would perceive as being an “ideal” analysis world, where we are free to assemble the individual building blocks as we need them and as they present themselves in terms of fitness, without any preconceived boundaries being applied. Our goal is to present a concept which is not only realistic in terms of physics, but also feasible in a contemporary sense.

Exemplary SN analysis:

We will begin with conducting a simple SN-analysis. As an example, we have chosen a polyacetal cantilever spring with dimensions provided in Fig. 25. The dimensions and material data have been supplied by DuPont [44].

$$L = 15.0 \text{ mm}$$

$$h = 2.54 \text{ mm}$$

$$b = 10.0 \text{ mm}$$

The spring will repeatedly be subjected to a deflection y of 0.75 mm. We wish to determine how many repeats the spring can withstand before it fractures.

We first determine the load W required to cause the deflection

$$L/h = 15.0/2.54 = 6.0$$

$$y/L = 0.75/15.2 \cong 0.05$$

Using the spring rate chart (see Fig. 26), we find the spring rate (W_c/y) by locating the intersection of the L/h and y/L lines. Thus, $W_c/y \cong 490 \text{ lbs/in.} = 85.8 \text{ N/mm}$. The load is therefore calculated as $W_c \cdot y = 85.8 \cdot 0.75 \cong 64.3 \text{ N}$. The chart was based on a spring width of 25.4 mm, meaning that we need to scale this result accordingly. Our load therefore equates to $64.3 \cdot 10/25.4 = 25.3 \text{ N}$.

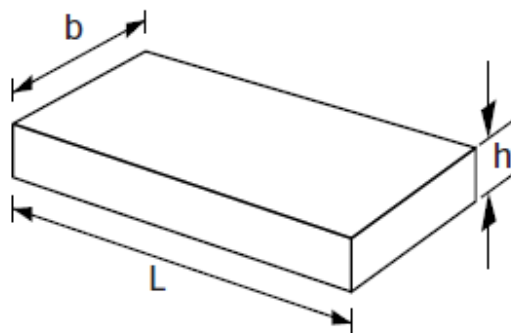


Figure 25: Dimension sketch for a cantilever spring.



The load can now be used to calculate the nominal bending stress, $\sigma_b = M_b/W_b$. Where M_b is the bending moment, W_b , and W_b the bending resistance, $bh^2/6$. The nominal bending stress is therefore $\sigma_b = 6 \cdot W \cdot L / bh^2 = 6 \cdot 25.3 \cdot 15 / 10 \cdot 2.54^2 \cong 35.3 \text{ N/mm}^2$, or MPa.

The number of repeats can now be extracted using the diagram shown in Fig. 27. The result is approximately 10^5 cycles before the spring fractures.

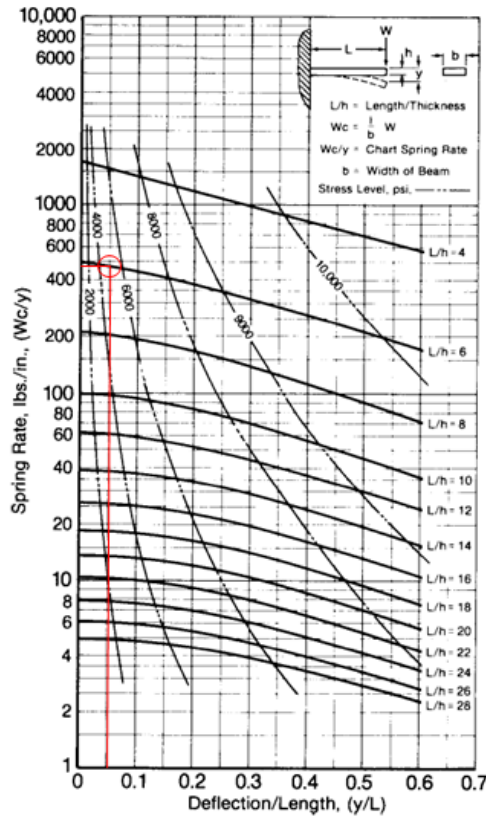


Figure 26: Spring rate chart for cantilever springs [44].

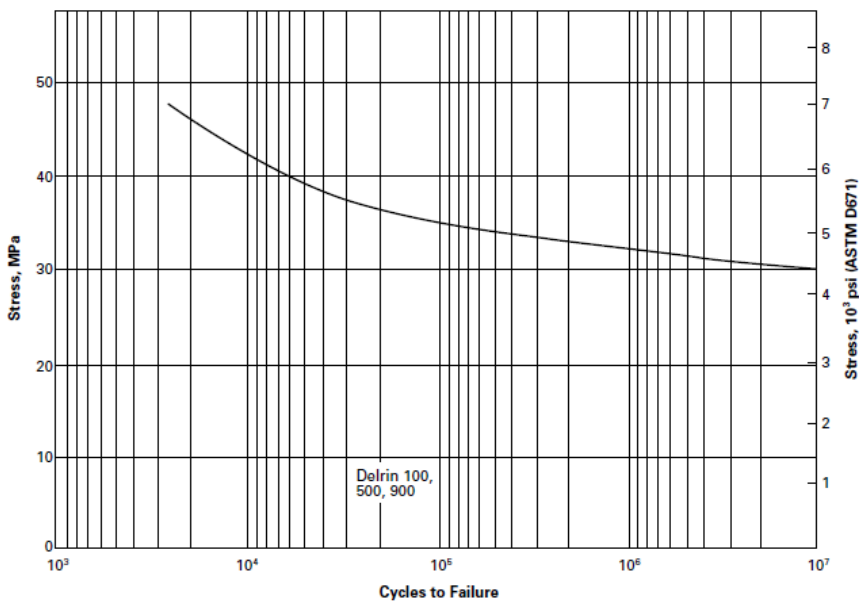


Figure 27: Flexural fatigue of Delrin POM [45].



DuPont [44] further provide the following advice regarding the design of springs:

“In the design of springs in Delrin® acetal resin, certain fundamental aspects of spring properties of Delrin® acetal resin should be recognized.

- *The effect of temperature and the chemical nature of the environment on mechanical properties.*
- *Design stresses for repeatedly operated springs must not exceed the fatigue resistance of Delrin® acetal resin under the operating conditions.*
- *Sharp corners should be avoided by provision of generous fillets.”*

This advice indirectly points out the shortcomings of the above analysis:

- The morphology can in no way be taken into account
 - The self-heating is not considered
- Local stress raisers are not taken into account
- SN data is provided for one temperature only and needs to be shifted for other relevant temperatures using an appropriate technique, unless more data can be measured.
- The approach becomes increasingly harder to justify with increasing geometrical complexity

SN analysis can in our opinion be considered a valid tool for comparing the infinite life margin of initial design variations, after which dedicated component analysis needs to follow once a design decision has been reached. That being said, without a proper temperature estimation technique, the concept will bear limited merit only.

Exemplary eN analysis:

Rather than trying to replicate the SN study, two strong limitations need to be pointed out. The first concerns the matter of cyclically stable stress-strain data. Through personal experience, the authors have been able to conclude that in spite of trying to resort to controlling measures during testing, the hysteresis loops in cyclic testing of plastics¹³ do not stabilize, even after intensely long periods of time. Kitagawa et. Al [46] report similar observations for PE, PP and POM.

The second limitation pertains to the process of deducing a Coffin-Manson type strain-life curve. To produce this diagram, uniaxial strain-controlled tests are necessary, where the strains are recorded for the most part using tactile devices. Uniaxial testing for anything but load-controlled pulsating tensile fatigue testing requires purpose-made specimens, which greatly increases cost and that are not available as off-the-rack supply from plastics manufacturers. In addition to the former, trying to measure strain using glued on gauges, results in the test recording a compound of the plastic and the adhesive (typically epoxy resin) [47]. Non-tactile measurements devices such as laser extensometers, or techniques such as speckled patterns and digital image correlation need to be applied to correctly capture the strains on the surface of the specimen. Herein lies the nature of the second impediment. The temperature on the surface will be drastically different from that of the bulk and will not be detected. We have so far concluded that cracks are more likely to form inside the bulk than initiate on the surface, and we therefore need to know the temperature at the core in order to feed any simulation with accurate material data. Due to the temperature gradient being very steep, the monotonic and cyclically stable (if indeed possible to obtain) stress-strain response would need to be captured at a multitude of temperatures and a sensible interpolation technique utilised that is capable of coping with the glass transition phenomenon in plastics.

Adding to the above limitations is the influence of self-heating and how this affects the test results, a fact that would also need to be taken into account. It is therefore our opinion that eN analysis is the most difficult concept to adapt or apply to non-reinforced plastics.

Exemplary da/dN analysis:

A plastic component made of POM is subjected to a cyclic pulsating load ranging between 1.0 and 0.1. The load applied causes stresses in a critical design element of maximum 50 MPa in magnitude. The stress cycle would therefore range from $0.1 \cdot 50$ to $1.0 \cdot 50$ MPa ($\Delta\sigma = \sigma_{\max} - \sigma_{\min} = 50 - 5 = 45$ MPa). The requirement is that the component must display a minimum endurance of $5 \cdot 10^5$ cycles. We want to estimate the maximum acceptable internal flaw size resulting from the manufacturing process for the component to fulfil this requirement.

For the following experiment, we will use Irwins theory, which states that there is only a small annulus around the crack which is plastic. This allows us to use the idea of the stress intensity factor, although in simplified form, meaning that for a physically true description of the problem, we will still need to look at actual energy release rates.

The first step is to calculate the critical flaw size (which would cause fracture to occur in a single cycle). This may be obtained from the following equation:

¹³ PA46, PA66 and POM



$$K = Y\sigma(\pi a)^{1/2}$$

In here K is the stress intensity factor, σ is the applied stress, a is the flaw size, and Y is a geometric function. Assuming $Y = 1$ we obtain

$$K = \sigma(\pi a)^{1/2}$$

From which we derive, using K_c from [48]

$$a_c = \left(\frac{K_c}{\sigma}\right)^2 \frac{1}{\pi} = \left(\frac{3.6}{50}\right)^2 \frac{1}{\pi} = 0.00165 \text{ m} = 1.65 \text{ mm}$$

Here the subscript c denotes “critical”. Throughout the time history, cracks initiating in the material will continue to grow until this critical size has been reached. Bearing in mind the life requirement of $5 \cdot 10^5$ cycles, the following equation [Crawford] can be used to estimate the size of the largest permissible flaw occurring in the volume before cyclic damage commences.

$$\frac{2}{YC_2(\Delta\sigma)^n \pi^{\frac{n}{2}}(2-n)} \left\{ a_c^{(1-n/2)} - a_i^{(1-n/2)} \right\} = N_f$$

Where C_2 is the crack growth rate from the Paris law diagram, n is the slope in a Paris law diagram, a_i is the initial crack size, which we are solving for, and a_c is the critical flaw size at which fracture occurs. From [48], we choose $C_2 = 8 \cdot 10^{-5}$, $n = 23.3$, and we already found $a_c = 1.65$ mm.

Rearranging our equation yields

$$a_c^{(1-n/2)} - N_f \frac{YC_2(\Delta\sigma)^n \pi^{\frac{n}{2}}(2-n)}{2} = a_i^{(1-n/2)}$$

And solving for a_i (provided $n \neq 2$)

$$a_i \rightarrow \left(a_c^{(1-n/2)} - \pi^{\frac{n}{2}} Y(\Delta\sigma)^n C_2 N_f + \frac{1}{2} n \pi^{\frac{n}{2}} Y(\Delta\sigma)^n C_2 N_f \right)^{\frac{2}{n-2}}$$

This function assumes that our geometric function Y does not change as the crack grows. This allows us to calculate $2a_i = 90 \mu\text{m}$. Based on this size we can determine by microscopic inspection, CT or other suitable technique whether or not a component will be able to survive a prescribed number of cycles from a perspective of serial production. A typical spherulite size for high quality processed polyacetal component typically ranges from 25 - 45 μm ¹⁴. The orders of magnitude in the above calculations thus appear realistic, which in turn indicates that a prediction of whether or not the required life can be achieved bears initial plausible merit.

The above approach does still not incorporate the thermal influence due to the frequency of loading. However, here factors are working in alternate directions. On the one hand, an increase in temperature will reduce the viscosity and hence the stress. This means that the change in stress intensity factor also decreases. On the other hand it is likely that the Paris parameters will shift as well. Considering the underlying fracture mechanics in play, it is likely that the amount of energy required to fracture will change in a moderate fashion while the temperature rises. Elevated temperatures will facilitate pull out, and thus the fracture energy can be expected to drop. The extent of this effect determines how temperature effects will need to be incorporated into the above approach. Clearly, the geometric function also needs further specification, rather than simply assuming it to be equal to 1.

At this stage, it is important to emphasize that Irwin’s idea was intended for materials with moderate plasticity zones. The experiment just conducted is thus promising, but will need some amount of adaptation. The authors are aware of the simplifications being made regarding the behaviour, but we have done so to show the workings of the da/dN idea as a concept.

¹⁴ From the authors personal experience.



It is clear that da/dN analysis seems to provide the largest potential for future physically founded fatigue analyses of plastics, but from all the points mentioned, it is also obvious that further research is necessary in this field.

CONCLUSIONS AND RECOMMENDATIONS

We have studied the morphological behaviour of plastics and seen that the material behaviour depends on the manufacturing process of the component. We also have seen that the temperature plays a crucial role in any material behaviour of plastics, and thus also in its fatigue behaviour.

We have given an overview of how classical fatigue algorithms could be applied, but have also shown that they will have difficulty predicting correct behaviour, because none of them directly incorporates the morphology and temperature predictions.

In order to come up with improved fatigue algorithms for plastics, we cannot just try and turn the knobs on the available fatigue algorithms for metals. These have clearly been devised to match metal response, and lack the characteristic behaviour observable in plastics. Fatigue algorithms are clever methods to attempt and match experimental results borne from pure phenomenological attempts of capturing certain experimental results into an equation, and some behavioural argumentation to extend the curve to multiaxiality and non-linear behaviour.

For both SN and eN algorithms it is assumed that nothing happens until a certain fatigue threshold is reached, which is not the case for plastics, since visco-elasticity/plasticity is always present. It is also assumed that although the order of loading is important, the speed of loading up until a reasonable limit is not too influential for the fatigue behaviour. This is yet another aspect which is clearly not the case for plastics, as we have demonstrated through the numerical experiment involving the temperature effect.

Temperature dependence in SN and eN algorithms are typically handled by taking the maximum temperature over the life span, and use that as a conservative estimate in obtaining life. In plastics this would nearly always lead to low cycle fatigue results, and we could not rely on ambient measurements of temperature in the first place, an analysis would have to be made.

In order to improve on this, the following points need to be considered.

- The injection moulding process needs to be simulated, prior to the FEA analysis to obtain a distribution of properties. This would provide the analyst with the skin effect, and the distribution of crystallinity. This would also justify the use of an energy-based approach, as this can describe the accumulation of actual damage.
- If we do not wish to make the whole fatigue analysis FEA-bound, that is, needing to perform a full thermomechanical FEA for each loading cycle, we need a simplified way to deal with the energy being released when going through the cycles. Some attempts in this direction have been made [Manson&Hertsberg]. However, they assume adiabatic conditions, which would lead to unrealistic high local heating, as they point out themselves. One would need a simplified equation to take into account both local heating, as well as diffusion and convection to the environment.
- The non-linear visco-elastic behaviour of the plastic would need to be taken into account using a methodology similar to a Ramberg-Osgood law, which in itself is not sufficient to capture the behaviour in a fatigue analysis.

The answer to an efficient solution to the problem fatigue of plastics is not yet out there, but if we take into account the understanding of the behaviour of plastics as discussed, we can at least make efficient stabs at the structure of a potentially successful solution, rather than trying to modify phenomenological models originally intended for a different class of materials.

REFERENCES

- [1] Doi, M., Introduction to Polymer Physics, Oxford University Press, (1996).
- [2] Doi, M., Edwards, F.S., The Theory of Polymer Dynamics, Oxford University Press, (1986).
- [3] Bird, R., Armstrong, R., Hassager, O., Dynamics of Polymeric Liquids - Fluid Mechanics, John Wiley and Sons, (1987).
- [4] Bird, R., Armstrong, R., Hassager, O., Dynamics of Polymeric Liquids - Kinetic Theory, John Wiley and Sons, (1987).
- [5] Elias, H-G., An Introduction to Plastics, Wiley VCH Verlag, (1997).
- [6] Ferry, J., Viscoelastic Properties of Polymers, John Wiley & Sons, (1980).



- [7] Schiefer, H., Beitrag zur Beschreibung des Zusammenhanges zwischen physikalischer Struktur und technischer Eigenschaft bei amorphem Polystyrol, Technische Hochschule Carl Scherlemmer Leuna-Merseburg, Diss., (1975).
- [8] Gruenwald, G., *Plastics: How Structure Determines Properties*, Carl Hanser Verlag, (1993).
- [9] Erhard, G., *Konstruieren mit Kunststoffen*, 1. Auflage, Carl Hanser Verlag, (1993).
- [10] Birley, W. A., Haworth, B., Batchelor, J., *Physics of Plastics*, Hanser Publishers, (1992).
- [11] VICTREX Plc., *Kristallinität und Morphologie*, Company Presentation, Victrex Plc., (2004).
- [12] Schulz, M. J., *Polymer Crystallization*, Oxford University Press, (2001).
- [13] Mandelkern, L., *Crystallization of Polymers - Equilibrium Concepts*, Cambridge University Press, (2002).
- [14] Mandelkern, L., *Crystallization of Polymers - Kinetics and Mechanisms*, Cambridge University Press, (2002).
- [15] Elias, H-G., *Makromoleküle Bd. 2*, Wiley VCH Verlag, (2001).
- [16] Michler, G. H., Baltá-Calleja, F. J. (Eds.), *Mechanical Properties of Polymers Based on Nanostructure and Morphology*, Taylor & Francis Group, (2005).
- [17] Hsiung, C., M., Cakmak, M., White, J., L.: *Structural Gradients in Injection Molded PPS*, *International Polymer Processing* 5 (1990) 2.
- [18] Hsiung, C., M., Cakmak, M., White, J., L., *Crystallization Phenomena in the Injection Molding of PolyEtherEtherKetone and its Influence on Mechanical Properties*, *Polymer Engineering and Science* 30 (1990).
- [19] Hsiung, C., M., Cakmak, M.: *Computer Simulations of Crystallinity Gradients Developed in Injection Molding of Slowly Crystallizing Polymers*, *Polymer Engineering and Science*, 31 (1991).
- [20] Hsiung, C., M., Cakmak, M.: *Effect of Processong Conditions on the Structural Gradients in Injection-Molded PAEK Parts - I. Characterization by Microbeam X-Ray Diffraction Technique*, *Journal of Applied Polymer Science*, 47 (1993).
- [21] Hsiung, C., M., Cakmak, M., *Effect of Processong Conditions on the Structural Gradients in Injection-Molded PAEK Parts - II. Large Dumbbell Parts* *Journal of Applied Polymer Science*, 47 (1993).
- [22] Ulcer, Y., Cakmak, M., Miao, J., Hsiung, C., M., *Structural Gradients developed in Injection-Molded Syndiotactic*
- [23] *Polystyrene (sPS)*, *Journal of Applied Polymer Science*, 60 (1996).
- [24] Menges, G., *Werkstoffkunde der Kunststoffe*, Carl Hanser Verlag, (1979).
- [25] Backhaus, J., *Gezielte Qualitätsvorhersage bei thermoplastischen Spritzgußteilen*, RWTH Aachen, Diss., (1985).
- [26] BASF AG (Hrsg.), *Konstruieren mit thermoplastischen Kunststoffen 5.93*, BASF, (1991).
- [27] Faatz, P., *Tribologische Eigenschaften von Kunststoffen im Modell- und Bauteilversuch*, Universität Erlangen-Nuernberg, Diss. (2002).
- [28] Wübken, G., *Einfluss der Verarbeitungsbedingungen auf die innere Struktur thermoplastischer Spritzgussteile unter besonderer Berücksichtigung der Abkühlverhältnisse*, RWTH Aachen, Diss., (1974).
- [29] Osswald, T.A., Menges, G., *Materials Science of Polymers for Engineers*, Carl Hanser Verlag, (2003).
- [30] Crawford, R.J., *Plastics Engineering*, Butterworth-Heinemann, (1998).
- [31] *Forschungskuratorium Maschinenbau (Hrsg.), Rechnerischer Festigkeitsnachweis für Maschinenbauteile aus Stahl, Eisenguss- und Aluminiumwerkstoffen*, VDMA Verlag, (2003).
- [32] Taylor, D., *The Theory of Critical Distances: A New Perspective in Fracture Mechanics*, Elsevier Science, (2007).
- [33] Susmel, L., *Multiaxial Notch Fatigue*, Woodhead Publishing, (2009).
- [34] Kanvinde, A.M., Deierlein, G.G., *Void Growth Model and Stress Modified Critical Strain Model to Predict Ductile Fracture in Structural Steels*, *Journal of Structural Engineering*, December (2006).
- [35] Kanvinde, A.M., Deierlein, G.G., *Cyclic Void Growth Model to Assess Ductile Fracture Initiation in Structural Steels due to Ultra Low Cycle Fatigue*, *Journal of Engineering Mechanics*, June (2007).
- [36] Kanvinde, A.M., Deierlein, G.G., *Validation of Cyclic Void Growth Model for Fracture Initiation in Blunt Notch and Dogbone Steel Specimens*, *Journal of Structural Engineering*, September (2008).
- [37] Cravero, S., Demarco, D., Klein, F., Ernst, H., *Ultra low cycle fatigue evaluation in notched geometries*, *Proc. of LCF7 – Seventh International Conference on Low Cycle Fatigue*, Aachen, (2013).
- [38] Michler, G.H., *Kunststoff-Mikromechanik*, Carl Hanser Verlag, (1998).
- [39] Kausch, H.H. (Ed.), *Crazing in Polymers*, Springer Verlag, (1983).
- [40] Kausch, H.H. (Ed.), *Crazing in Polymers*, Springer Verlag, 2 (1990).
- [41] Michler, G.H., *Electron Microscopy of Polymers*, Carl Hanser Verlag, (1998).
- [42] Böhme, E., *Failure Analysis using Microscopic Techniques*, DuPont Engineering Polymers, Geneva, (1990).
- [43] Baehr, H.D., *Thermodynamik: Grundlagen und technische Anwendungen*, Springer Verlag, (2005).
- [44] Shaw, T.M., MacKnight, W.J., *Introduction to Polymer Viscoelasticity*, John Wiley & Sons, (2005).
- [45] DuPont de Nemours and Company, *General Design Principles for DuPont Engineering Polymers*, Geneva, (1995).



- [46] DuPont de Nemours and Company, Delrin acetal resing Design Guide – Module III, Geneva, (2000).
- [47] Kitagawa, M., Qui, J., Nishida, K., Yoneyama, T., Cyclic stress-strain curves at finite strains under high pressures in crystalline polymers, *Journal of Materials Science*, 27 (1992).
- [48] Vallance, L., The Influence of Temperature on Damage Accumulation in Cyclically-loaded Non-reinforced Engineering Plastics, The University of Sheffield, M.Sc. thesis. (2014).
- [49] Bretz, P.E., Hertzberg, R.W., Manson, J.A., The Effect of Molecular Weight on Fatigue Crack Propagation in Nylon 66 and Polyacetal, *Journal of Applied Polymer Science*, 27 (1982).